

Effect of Low Temperature Annealing on Anatase TiO₂ Layer as Photoanode for Dye-Sensitized Solar Cell

Abstract. Dye-Sensitized Solar Cells (DSSCs) have been successfully fabricated with a low annealing temperature (100 °C to 500 °C) approach to the anatase TiO₂ photoanode deposited by a screen-printing method. In this paper, the surface morphology and structure of the TiO₂ thin films were studied using Scanning Electron Microscope (SEM), X-Ray Diffraction (XRD) and Raman Spectroscopy while I-V characteristic was used for the electrical properties. Sample with an annealing temperature of 300 °C displays a good feature in terms of porosity and enhanced agglomerated surface.

Streszczenie. Ogniwa słoneczne uczulone barwnikiem (DSSC) zostały z powodzeniem wyprodukowane przy niskiej temperaturze wyżarzania (100 °C do 500 °C) z fotokomórką anatazu TiO₂ osadzaną metodą sitodruku. W artykule zbadano morfologię powierzchni i strukturę cienkich warstw TiO₂ przy użyciu skaningowego mikroskopu elektronowego (SEM), dyfrakcji promieniowania rentgenowskiego (XRD) i spektroskopu Ramana, natomiast dla właściwości elektrycznych wykorzystano charakterystykę I-V. Próbkę o temperaturze wyżarzania 300 °C wykazuje dobrą cechę pod względem porowatości i zwiększonej powierzchni zaglomerowanej. (Wpływ wyżarzania niskotemperaturowego na warstwę TiO₂ jako fotoanodę w ogniwach słonecznych uczulonych na barwnik)

Keywords: Anatase TiO₂, Annealing Temperature, Dye-Sensitized Solar Cell, Surface Morphology.

Słowa kluczowe: Anatase TiO₂, Temperatura wyżarzania, Ogniwo słoneczne światłoczułe, Morfologia powierzchni.

Introduction

Dye-Sensitized Solar Cell (DSSC) is an emerging technology and has attracted a lot of attention among researchers due to its simple and low-cost fabrication process [1]. The cell is based on semiconductor material and made up of three basic layers of a photo-sensitized anode, a photo electrochemical system and an electrolyte [2]. DSSC is economically viable and practical as it is only needing one type of semiconductor as a charge carrier transport compared to the conventional p-n junction solar cell, that required multiple type of semiconductors for light absorption and charge carrier transport. DSSC was first introduced by Gratzel et al. that consists of three main part structures, transparent conductive oxide coating (ITO or FTO), a semiconductor oxide film deposited on the conductive side of the glass sheet and a mixture of a sensitizer and an electrolyte [3].

Basically, photovoltaic is a converting process of light energy into electrical energy [3–5]. Sunlight will release particles of light known as photons where it will pass through the transparent anode. Then, the dye molecule will be excited and consequently oxidized. The oxidized dye molecule will inject electron into the conduction band of TiO₂ layer which acts as a semiconductor [7]. Next, the electron flow to the electrode cathode and iodide electrolyte layer through the external circuit. After that the electron is transfer back to the working electrode by redox reaction through electrolyte [8].

Titanium dioxide (TiO₂) is widely used as photoanode of DSSCs due to its stability and non-toxicity material. In addition, this material is also abundant hence, economically feasible. The TiO₂ can be categorized into 3 types namely anatase, rutile and brookite but the most widely used as a photoanode is anatase. Anatase is widely chosen as photo catalysts due to its high photo activity [8,9]. In addition, anatase phase has a high surface area so it can transfer more electrons compared other type such as rutile [11]. Previous researches have proved that the annealed TiO₂ is the most effective and suitable material for photoanode due to its cost effective, good stability, compatible optical and electronic properties [11–13]. As a results, the TiO₂

produces a significant role increasing the photo-conversion efficiency reaching up to 12-14% of cell efficiency [15]. Photoanode is defined as the anode of the photoelectric cell and working electrode in DSSC also as a charge separator and a bridge [16].

The phase of TiO₂ change depends on the annealing temperature performed after the thin film deposition process. Initially, as-deposited TiO₂ is in amorphous phase and the structure begin to react or crystallized during annealing process at a temperature range between 300 °C to 600 °C [16,17]. Above these range, the TiO₂ phase will change to rutile phase due to metastable [19]. Metastable states develop kinetically in crystal growth reactions without reaching a stable state due to the overly strong chemical bonds. From this point of view, the TiO₂ phase depends on which phase grows faster as the crystalline nucleus during the polymerization of the TiO₆ octahedral unit. Zigzag packing is a crystal structure for anatase that generated from the octahedral TiO₆ unit configuration. Zigzag packing uses only the octahedral cis-coordination site for crystal growth; therefore, the probability is high for the occurrence of cis-coordination polymerization leading to metastable states in formation of anatase phase TiO₂ [18–20]. So, the state of TiO₂ material is influenced by the low annealing temperature which is below 550 °C. By reducing the annealing temperature, the flexible plastic substrate can be utilized for uneven surfaces. Moreover, the evaporation of the acetic acid as the solvent during the deposition will cause the surface of the TiO₂ become rougher as the annealing temperature increase [22]. This is because irregular structures will form when the solvent escapes from the film and it evaporates rapidly as the annealing temperature increases resulting in increased porosity and reduced density [23]. Besides, the surface morphology and crystallinity of TiO₂ thin film can be optimized by annealing process as it influence the electron transportation rate and effective surface area [24]. The annealing temperature allows the coefficient of electron diffusion and the lifetime of the electron to increase and at the same time results in more efficient transport of the electron in the photoelectrode. However, an increase in annealing

temperature will affect the adsorption of dye molecules as well as light harvesting due to the reduced internal surface area of the nanoparticles [25].

Solar cell performance is measured based on many criteria, but the cell efficiency is the key parameter to show the percentage of sunlight converted to electrical energy per area [25,26]. The efficiency of solar cells is calculated by the ratio of maximum output power to the input energy of the sun [28]. Moreover, the fraction of incident power converted to electricity lead to the production efficiency of solar cells. Equation 1 and 2 show the mathematical definition of efficiency where efficiency is expressed in percentage and P_{in} stands for input power from sunlight.

$$(1) \quad P_{max} = V_{OC} I_{SC} FF$$

$$(2) \quad Efficiency = \frac{P_{max}}{P_{in} \times Area}$$

where: P_{max} – maximum power, V_{OC} – open circuit voltage, I_{SC} – short circuit current, P_{in} – input power.

Besides, the fill factor (FF) is defined as the ratio of the maximum solar cell power to the product of V_{OC} and I_{SC} [28]. The fill factor does not have a unit since the ratio has the same physical parameter. Also, a higher fill factor can be obtained by increasing shunt resistance [28,29]. Equation 3 shows the mathematical definition of fill factor as V_{max} and I_{max} are the voltage and current at the maximum power.

$$(3) \quad Fill\ Factor = \frac{I_{max} \times V_{max}}{I_{SC} \times V_{OC}}$$

where: I_{max} – maximum current, V_{max} – maximum voltage.

Here we focus on the effect of the low temperature annealing on anatase TiO_2 thin film. The TiO_2 thin films were annealed at a different temperature in a range of 100 °C to 500 °C. Scanning Electron Microscope (SEM), X-Ray Diffraction (XRD) and Raman Spectroscopy characterization were performed to study the morphology and structure of the TiO_2 thin films [31–33]. Then I-V measurement was applied on the fully fabricated devices for the electrical characteristics.

Methodology

Indium Tin Oxide (ITO) coated glass with a dimension of 2.5 cm by 2.5 cm was used as a substrate in this work. The substrates were immersed into acetone and then ethanol for 10 min respectively by using ultrasonic bath to remove any organic contaminant on the substrates. Then the conductive side of the ITO glass was verified to confirm the ITO layer on the glass. TiO_2 paste was prepared by mixing 2 g of Sigma-Aldrich TiO_2 anatase powder with 2 ml of acetic acid in a mortar. The mixture is grinded using a pestle for 5 min and produced a well-blend compound. Then the mixture was deposited on the ITO glass using a screen printer producing a 10 μm thick of TiO_2 thin film layer.

After the TiO_2 layer deposition, the samples were immediately annealed. The samples were annealed at different temperatures in the range of 100 °C and 500 °C to observe the effect of annealing temperature on the anatase TiO_2 thin film. The sample was divided into two sets in which the first set of samples was annealed on a hot plate at 100 °C and 200 °C. Then the later set was annealed in the hot tube furnace with a temperature above 300 °C. Both processes are started after the desired temperature is reached and performed for 30 min to make a fair comparison. After the annealing process, the samples were cooled down for an hour under normal room ventilation. Then, a few drops of the extracted dye were dripped onto

the TiO_2 thin film and left for 30 min. In this paper, the dye extracted was obtained from 10 mg of Curcuma Longa (fine turmeric) soaked in 10 ml of ethanol for 24 hours.

For the counter electrode preparation, the conductive side of another cleaned ITO glass is passed through a candle flame several times. The redox shuttle and electrolyte were prepared by stirring 127 mg iodine crystal with 830 mg potassium iodide and diluted in 10 ml ethylene glycol. In the final assembly, a few drops of electrolyte were dispensed into the stained sample and sandwiched it with the soot-covered slide. The layered parts then face each other with excessive exposure on both sides for the purpose of electrical measurement. The surface morphology is characterized using Expert Pro PANalytical PRO MPD X-Ray Diffraction (XRD), UniRAM 3500 Raman Spectroscopy and Carl Zeiss Evo 50 Scanning Electron Microscope (SEM).

Result and Discussion

The anatase TiO_2 thin film DSSC has been fully fabricated and has converted the sunlight into electrical energy. The surface morphology and electrical characteristic measurement have been performed to study the effect of the annealing process to the cell.

a) X-Ray Diffraction (XRD)

The surface profile of anatase TiO_2 thin film is characterized using XRD, Raman Spectroscopy and SEM. Fig. 1 shows the XRD pattern of deposited anatase TiO_2 nanoparticle annealed at 300 °C. Based on the spectrum peaks, it can be confirmed that the deposited TiO_2 thin film layer is in anatase phase. Ten peaks (JCPDS: No. 00-021-1272) labeled with a plane value in the graph are proportional to the anatase plane appeared at 25.3 °, 30.2 °, 31.6 °, 36.9 °, 37.7 °, 38.6 °, 48 °, 53.9 °, 55 °, 60.2 ° and 62.7 ° respectively. Besides, the rutile peak (JCPDS: No. 00-004-0551) is also detected, at 27.4 ° with (110) plane value. However, this value is too small to be considered compared to significant anatase phase peaks. In addition, two pronounced peaks (JCPDS: No. 00-021-1236) can be indexed to the (400) and (441) reflections indicating ITO glass were also found at 2 theta values of 35 ° and 50.6 ° respectively. The JCPDC data file from the X-Pert software is used as reference to the peak values for all material [34]. The strength peak showed the number of atoms containing the sum of electrons in the unit cell of the analyzed material [35]. Hence, at 25.3 ° theta, the largest number of atoms and containing the highest volume of an electron in the unit cell is confirmed to be the anatase TiO_2 thin film. The spectra also display that the TiO_2 thin film layer are crystallized after the annealing process. This is most probably due to the annealing process and added with the usage of Sigma Aldrich pure anatase TiO_2 powder.

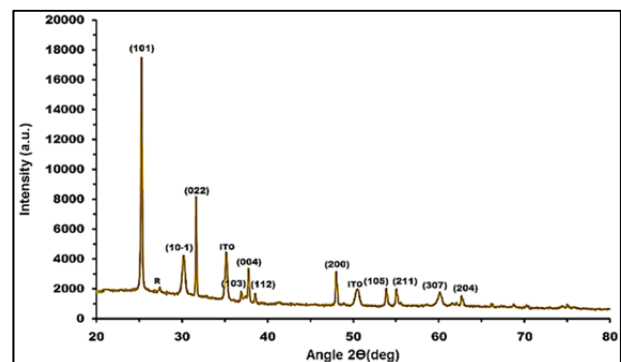


Fig.1. X-RD pattern of anatase TiO_2 nanoparticle.

b) Raman Spectroscopy

In addition, the samples were also analysed using Raman spectroscopy to study the vibrational mode of TiO₂ thin film. Fig 2. shows the strong Raman peaks obtained in this work were found at 128 cm⁻¹, 182 cm⁻¹, 378 cm⁻¹, 500 cm⁻¹ and 621 cm⁻¹. These peaks are very close to the peak obtained in the previous study which are set as Eg, Eg, B1g, A1g+B1g and Eg modes of anatase phase. Previous studies stated that, there are six active modes of Raman (A1g+2B1g+3Eg) in the anatase phase where the intensity at (144 cm⁻¹, 197 cm⁻¹, 639 cm⁻¹)Eg, (399 cm⁻¹, 519 cm⁻¹)B1g and (513 cm⁻¹)A1g over the Raman shift [32–34]. Raman shift is the frequency difference between laser light and scattering light and it is also associated with the length of chemical bonds in particles [35,36]. As the Raman shift increases, the length of the chemical bond will decrease and vice versa. A strong peak found at 128 cm⁻¹ mode shows the highest amount of anatase content and asserts that the TiO₂ nanoparticle has a certain degree of long-range order [37,38]. Moreover, the lightest and prominent anatase atomic bond is occurs at the Raman shift of 621 cm⁻¹ due to the short length of the chemical bonding. In addition, all of the peaks are also broadened due to participate of the phonon other than Brillouin zone centre and influence of confined phonons or surface pressure derived from the materials in nanometre regime [37,38]. Due to the spatial confinement of phonons in the nanometre regime, the phonons outside the centre of the Brillouin zone are involved in the Raman scattering phase due to the relaxation of the phonon momentum selection rules of q = 0 occurring at the bulk level [43]. The number of Raman waves and the broadening lines that produce an upward or downward shift depending on whether the transverse optical mode (TO) propagation has a positive or negative curvature.

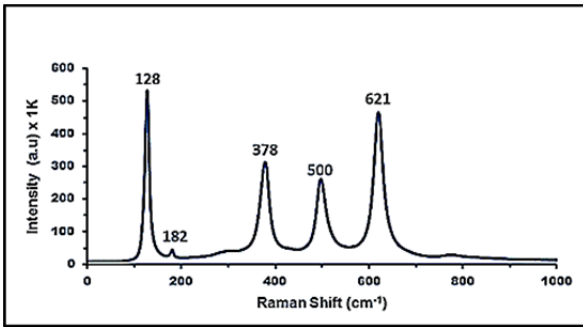


Fig.2. Raman Spectrum of TiO₂ anatase material.

c) Scanning Electron Microscope (SEM)

The porosity and density of the structure can be analyzed by the SEM device [44]. SEM images for TiO₂ thin film annealed at various temperatures of 100 °C, 200 °C, 300 °C, 400 °C and 500 °C are shown in Fig. 3(a) - (e) with magnification factor of ×5000. From the scanned images, it is observed that all samples possess a mesoporous structure with particles diameter in nanometre regime, indicating that it is naturally perfect for the absorption of dye into the surface. It is also observed that, as the annealed temperature rises, the porosity structure and the density of the TiO₂ particle increases [18]. Samples with an annealing temperature of 300 °C was found to have a better structure than others due to their porous surface, and the structure appeared to be more agglomerated.

In addition, SEM images for TiO₂ thin film annealed at temperature 300 °C with increased magnification factors from ×19 to ×7000 are shown in Fig 4 (a) - (e). Fig 4(b) with magnification factor ×79 shows that the surface shape of

the TiO₂ layer is not uniform, this may be due to the poor handling during the deposition process. However, it is clearly observed that the thin film structure has a high porosity and agglomerated which increase the light scattering absorption as depicted in Fig 4(e).

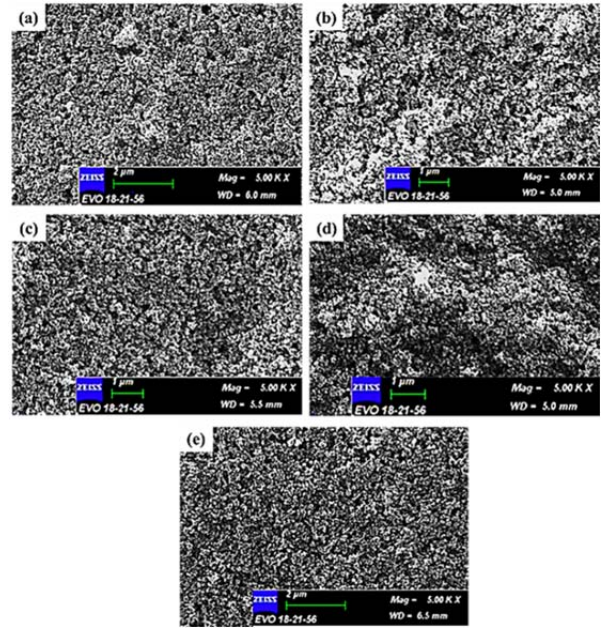


Fig.3. SEM images of TiO₂ thin film annealed at (a) 100 °C, (b) 200 °C, (c) 300 °C, (d) 400 °C, and (e) 500 °C for 30 min.

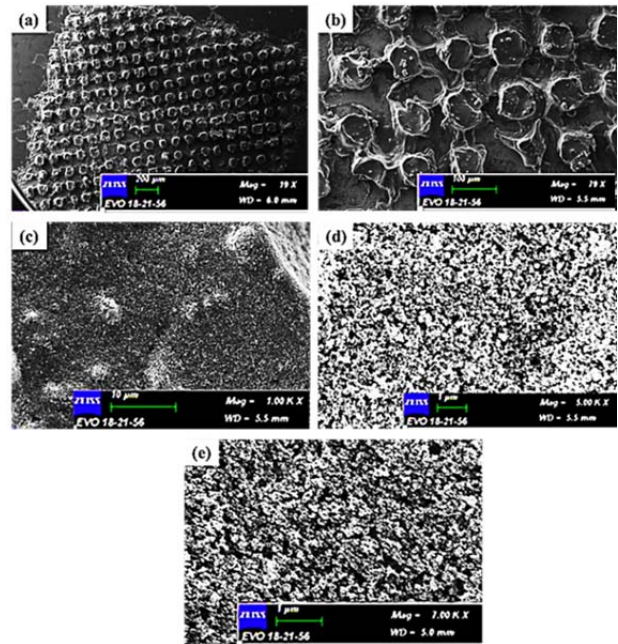


Fig.4. SEM image of TiO₂ thin film annealed at 300 °C for 30 min with magnification factor of (a) × 19, (b) × 79, (c) × 1000, (d) × 5000, and (e) × 7000.

d) Electrical Measurement

Table 1 shows the current and voltage measurement of samples determined under sunlight with various annealing temperatures in a range between 100 °C to 500 °C. The current is measured using a probe station at certain bias voltage. Based on the electrical results, the best produced energy is sample 3 which was annealed at 300 °C. This indicate that the IV characteristic of anatase TiO₂ thin film is greatly influenced by the different annealing temperature. In

addition, this results also shows that the anatase TiO₂ thin film starts to crystallize at 300 °C, similar to the previous works by Muaz et al. [17,41,42].

Table 1. Electrical Properties of DSSC

Sample	Annealing Temperature (°C)	Current (µA)	Voltage (mV)
S1	100	65	126
S2	200	45	322
S3	300	36	490
S4	400	41	183
S5	500	33	161

Conclusion

We fabricated complete DSSC with TiO₂ thin film as photoanode using screen printing technique. The deposited TiO₂ thin film were then annealed in different temperature to study the effect of annealing process. From surface morphology results, all the samples demonstrated a well structure of anatase phase verified by XRD measurement. From the SEM images it is observed that all TiO₂ particles are naturally possess a mesoporous structure which is good for the absorption of the dye into the surface. In addition, visually it can be seen that the porosity structure and the distance between the TiO₂ particles increase with increasing annealing temperature. At annealing temperature of 100 °C, it was observed that there were many cavities produced and the porous structure was still unsatisfactory whereas for annealing temperature at 200 °C showed that the number of cavities decreased, and the structure appeared slightly lumpy. However, the sample with annealing temperature of 300 °C has shown a high porosity level and more agglomerated. These features would enhance the light scattering absorption and thus increase the solar cell efficiency. The IV characteristics measurement also displays that sample with annealing temperature of 300 °C has produced the best electrical energy in term of current and voltage. The TiO₂ layer began to crystallize at 300 °C and this finding has been supported by previous research [18]. Moreover, this is the first report for such temperatures using screen printing technique. As manufacturing costs to produce solar cells increase dramatically, this work could be an alternative to replace the conventional techniques [47].

Acknowledgement

This work was supported by Universiti Teknikal Malaysia Melaka and Ministry of Education Malaysia under RACER/2019/FKEKK-CETRI/F00403.

Authors: Nur Syamimi Nooraid, Centre for Telecommunication Research & Innovation, Faculty of Electronic and Computer Engineering, Universiti Teknikal Malaysia Melaka, Hang Tuah Jaya, 76100, Durian Tunggal, Malaysia, Email: m022010022@student.utm.edu.my; Faiz Arith, Centre for Telecommunication Research & Innovation, Faculty of Electronic and Computer Engineering, Universiti Teknikal Malaysia Melaka, Hang Tuah Jaya, 76100, Durian Tunggal, Malaysia, E-mail: faiz.arith@utm.edu.my.; Ahmad Nizamuddin Mustafa, Centre for Telecommunication Research & Innovation, Faculty of Electrical and Electronic Engineering Technology, Universiti Teknikal Malaysia Melaka, Hang Tuah Jaya, 76100, Durian Tunggal, Malaysia, E-mail: nizamuddin@utm.edu.my; Mohd Asyadi Azam, Faculty of Manufacturing Engineering, Universiti Teknikal Malaysia Melaka, Hang Tuah Jaya, 76100, Durian Tunggal, Malaysia, E-mail: asyadi@utm.edu.my; Syazwan Hanani Meriam Suhaimy, Faculty of Applied Sciences and Technology Universiti Tun Hussein Onn Malaysia Johor, Malaysia, E-mail: hananie@uthm.edu.my; Oras A Al-Ani, Electrical Engineering Technical College, Middle Technical University, Baghdad, Iraq, Email: dr.oras@eetc.mtu.edu.iq

REFERENCES

- [1] Nooraid N.S., Arith F., Alias S.N., Mustafa A.N., Roslan H., Johari S.H., Rahim H.R.A., Ismail M.M., Synthesis of ZnO Nanorod Using Hydrothermal Technique for Dye-Sensitized Solar Cell Application. In: *Intelligent Manufacturing and Mechatronics*: Springer, Singapore, 2021, 895–905
- [2] Zulkifli A.N.B., Kento T., Daiki M., Fujiki A., The Basic Research on the Dye-Sensitized Solar Cells (DSSC), *Journal of Clean Energy Technologies*, 3 (2014), Nr. 5, 382–387
- [3] Polizzotti A., Schual-Berke J., Falsgraf E., Johal M., Investigating New Materials and Architectures for Grätzel Cells. In: *Third Generation Photovoltaics*, 2012
- [4] Maciej Łuszczek, Grzegorz Łuszczek D., Simulation investigation of perovskite-based solar cells, *Przegląd Elektrotechniczny*, 97 (2021), Nr. 5, 99–102
- [5] Tivanov M., Moskalev A., Kaputskaya I., Żukowski P., Calculation of the ultimate efficiency of p-n-junction solar cells taking into account the semiconductor absorption coefficient, *Przegląd Elektrotechniczny*, 92 (2016), Nr. 8, 85–87
- [6] Arafat Azidin F., Hannan M.A., Mohamed A., Renewable Energy Technologies and Hybrid Electric Vehicle Challenges, *Przegląd Elektrotechniczny*, 89 (2013), Nr. 8, 150–156
- [7] Arith F., Anis S.A.M., Said M.M., Idris C.M.I., Low cost electro-deposition of cuprous oxide P-N homo-junction solar cell, *Advanced Materials Research*, 827 (2014), 38–43 — ISBN 9783037859001
- [8] Gratzel M., Dye-sensitized solar cells, *Journal of Photochemistry and Photobiology C: Photochemistry Reviews*, 4, Elsevier (2003), Nr. 2, 145–153
- [9] Meriam Suhaimy S.H., Ghazali N., Arith F., Fauzi B., Enhanced simazine herbicide degradation by optimized fluoride concentrations in TiO₂ nanotubes growth, *Optik*, 212 (2020), 164651
- [10] Bakardjieva S., Subrt J., Stengl V., Dianez M.J., Sayagues M.J., Photoactivity of anatase-rutile TiO₂ nanocrystalline mixtures obtained by heat treatment of homogeneously precipitated anatase, *Applied Catalysis B: Environmental*, 58 (2005), Nr. 3–4, 193–202
- [11] Park N.-G., van de Lagemaat J., Frank A.J., Comparison of Dye-Sensitized Rutile- and Anatase-Based TiO₂ Solar Cells, *The Journal of Physical Chemistry B*, 104 (2002), Nr. 38, 8989–8994
- [12] Dette C., Pérez-Osorio M.A., Kley C.S., Punke P., Patrick C.E., Jacobson P., Giustino F., Jung S.J., Kern K., TiO₂ anatase with a bandgap in the visible region, *Nano Letters*, 14 (2014), Nr. 11, 6533–6538
- [13] Asahi R., Taga Y., Mannstadt W., Electronic and optical properties of anatase, *Physical Review B - Condensed Matter and Materials Physics*, 61 (2000), Nr. 11, 7459–7465
- [14] Humayun M., Raziq F., Khan A., Luo W., Modification strategies of TiO₂ for potential applications in photocatalysis: A critical review, *Green Chemistry Letters and Reviews*, 2 (2018), Nr. 11, 86–102
- [15] N. A. Ludin, A. M. Ramli M.Z.R., Performance Enhancement of Dye Sensitized Solar Cell Using Graphene Oxide Doped Titanium Dioxide Photoelectrode, *Malaysian Journal of Analytical Science*, 21 (2017), 928–940
- [16] Mansa R.F., Yugis A.R.A., Liow K.S., Chai S.T.L., Ung M.C., Dayou J., Sipaut C.S., A brief review on photoanode, electrolyte, and photocathode materials for dye-sensitized solar cell based on natural dye photosensitizers. In: *Developments in Sustainable Chemical and Bioprocess Technology*, 2013 — ISBN 9781461462088, 313–319
- [17] Abdulraheem Y.M., Ghoraiishi S., Arockia-Thai L., Zachariah S.K., Ghannam M., The effect of annealing on the structural and optical properties of titanium dioxide films deposited by electron beam assisted PVD, *Advances in Materials Science and Engineering*, (2013)
- [18] Muaz A.K.M., Hashim U., Ibrahim F., Thong K.L., Mohktar M.S., Liu W.W., Effect of annealing temperatures on the morphology, optical and electrical properties of TiO₂ thin films synthesized by the sol-gel method and deposited on Al/TiO₂/SnO₂/p-Si, *Microsystem Technologies*, 22 (2016), Nr. 4, 871–881
- [19] Satoh N., Nakashima T., Yamamoto K., Metastability of anatase: Size dependent and irreversible anatase-rutile phase transition in atomic-level precise titania, *Scientific Reports*, 3 (2013), 1959

- [20] Kumar S.G., Rao K.S.R.K., Polymorphic phase transition among the titania crystal structures using a solution-based approach: From precursor chemistry to nucleation process, *Nanoscale*, 6 (2014), Nr. 20
- [21] Verma R., Gangwar J., Srivastava A.K., Multiphase TiO₂ nanostructures: A review of efficient synthesis, growth mechanism, probing capabilities, and applications in bio-safety and health, *RSC Advances*, 7 (2017), Nr. 70, 44199–44224
- [22] Fazli F.I.M., Ahmad M.K., Soon C.F., Nafarizal N., Suriani A.B., Mohamed A., Mamat M.H., Malek M.F., Shimomura M., Murakami K., Dye-sensitized solar Cell using pure anatase TiO₂ annealed at different temperatures, *Optik*, 140 (2017), 1063–1068
- [23] Zhou S., Zhang J., Fang Z., Ning H., Cai W., Zhu Z., Liang Z., Yao R., Guo D., Peng J., Thermal effect of annealing-temperature on solution-processed high- κ ZrO₂ dielectrics, *RSC Advances*, 9 (2019), Nr. 22, 42415–42422
- [24] Zhao D., Peng T., Lu L., Cai P., Jiang P., Bian Z., Effect of annealing temperature on the photoelectrochemical properties of dye-sensitized solar cells made with mesoporous TiO₂ nanoparticles, *Journal of Physical Chemistry C*, 112 (2008), Nr. 22, 8486–8494
- [25] Xi J., Dahoudi N. Al, Zhang Q., Sun Y., Cao G., Effect of annealing temperature on the performances and electrochemical properties of TiO₂ dye-sensitized solar cells, *Science of Advanced Materials*, 4 (2012), Nr. 7, 727–733
- [26] El amine Aichouba M., Rahli M., Solar cell parameters extraction optimization using Lambert function, *Przegląd Elektrotechniczny*, 95 (2019), Nr. 4, 227–231
- [27] Sredenšek K., Seme S., Parameter determination of a solar cell model using differential evolution algorithm, *Przegląd Elektrotechniczny*, 95 (2019), Nr. 1
- [28] Azhari M.A., Arith F., Ali F., Rodzi S., Karim K., Fabrication of low cost sensitized solar cell using natural plant pigment dyes, *ARNP Journal of Engineering and Applied Sciences*, 10 (2015)
- [29] Leilaieoun M., Holman Z.C., Accuracy of expressions for the fill factor of a solar cell in terms of open-circuit voltage and ideality factor, *Journal of Applied Physics*, 120 (2016), Nr. 12, 123111
- [30] Qi B., Wang J., Fill factor in organic solar cells, *Physical Chemistry Chemical Physics*, 15 (2013), 8972–8982
- [31] Asyadi Azam M., Ezyanie Safie N., Fareezuan Abdul Aziz M., Noor Amalina Raja Seman R., Rafi Suhaili M., Abdul Latiff A., Arith F., Mohamed Kassim A., Hanafi Ani M., Structural characterization and electrochemical performance of nitrogen doped graphene supercapacitor electrode fabricated by hydrothermal method, *International Journal of Nanoelectronics and Materials (IJNeM)*, 14 (2021), Nr. 2, 127–136
- [32] Aliyaselvam O. V., Arith F., Mustafa A.N., M. K. N., Al-Ani O., Solution Processed of Solid State HTL of CuSCN Layer at Low Annealing Temperature for Emerging Solar Cell, *International Journal of Renewable Energy Research-IJREER*, 11 (2021), Nr. 2, 10
- [33] Chelvanathan P., Shahahmadi S.A., Arith F., Sobayel K., Aktharuzzaman M., Sopian K., Alharbi F.H., Tabet N., Amin N., Effects of RF magnetron sputtering deposition process parameters on the properties of molybdenum thin films, *Thin Solid Films*, 638, Elsevier B.V. (2017), 213–219
- [34] Morris M.C., McMurdie H.F., Evans E.H., Paretzkin B., Parker H.S., Pyrrros N.P., Hubbard C.R., Standard X-Ray Diffraction Powder Patterns., *NBS Monograph (United States)*, (1982)
- [35] Roller J., X-ray diffraction. In: *PEM Fuel Cell Diagnostic Tools*, 2011 — ISBN 9781439839201, 289–313
- [36] Ohsaka T., Izumi F., Fujiki Y., Raman spectrum of anatase, TiO₂, *Journal of Raman Spectroscopy*, 7 (1978), 321–324
- [37] Mathpal M.C., Tripathi A.K., Singh M.K., Gairola S.P., Pandey S.N., Agarwal A., Effect of annealing temperature on Raman spectra of TiO₂ nanoparticles, *Chemical Physics Letters*, 555 (2013), 182–186
- [38] Cheng G., Akhtar M.S., Yang O.B., Stadler F.J., Structure modification of anatase TiO₂ nanomaterials-based photoanodes for efficient dye-sensitized solar cells, *Electrochimica Acta*, 113 (2013), 527–535
- [39] Yang X.X., Li J.W., Zhou Z.F., Wang Y., Yang L.W., Zheng W.T., Sun C.Q., Raman spectroscopic determination of the length, strength, compressibility, Debye temperature, elasticity, and force constant of the C-C bond in graphene, *Nanoscale*, 4 (2012), 502–510
- [40] Colomban P., Gouadec G., Raman Scattering Theory and Elements of Raman Instrumentation. In: *Raman Spectroscopy for Soft Matter Applications*, 2008 — ISBN 9780470453834, 11–29
- [41] Gupta S.K., Desai R., Jha P.K., Sahoo S., Kirin D., Titanium dioxide synthesized using titanium chloride: Size effect study using Raman spectroscopy and photoluminescence, *Journal of Raman Spectroscopy*, 41 (2010), 350–355
- [42] Musila N., Munji M., Simiyu J., Masika E., Nyenge R., Kineene M., Characteristics of TiO₂ Compact Layer prepared for DSSC application, *Path of Science*, 4 (2018), Nr. 10, 3006–3012
- [43] Arora A.K., Rajalakshmi M., Ravindran T.R., Sivasubramanian V., Raman spectroscopy of optical phonon confinement in nanostructured materials, *Journal of Raman Spectroscopy*, 38 (2007), 604–617
- [44] Nizamuddin A., Arith F., Rong I.J., Zaimi M., Rahimi A.S., Saat S., Investigation of Copper(I) Thiocyanate (CuSCN) as a Hole Transporting Layer for Perovskite Solar Cells Application, *Journal of Advanced Research in Fluid Mechanics and Thermal Sciences*, 78 (2021), Nr. 2, 153–159
- [45] Yanagisawa K., Ovenstone J., Crystallization of anatase from amorphous titania using the hydrothermal technique: Effects of starting material and temperature, *Journal of Physical Chemistry B*, 103 (1999), Nr. 37, 7781–7787
- [46] Benčina M., Igljič A., Mozetič M., Junkar I., Crystallized TiO₂ nanosurfaces in biomedical applications, *Nanomaterials*, 10 (2020), Nr. 6, 1121
- [47] Shakeel Ahmad M., Pandey, A. K., Abd Rahim N., Advancements in the development of TiO₂ photoanodes and its fabrication methods for dye sensitized solar cell (DSSC) applications. A review, *Renewable and Sustainable Energy Reviews*, 77 (2017), 89–108